Comparative Study of Trapezoïdal And Sinusoïdal Control of Electric Vehicle Power Train

Souhir Tounsi

Abstract— The production of the electric vehicles is always braked by their weak autonomies and their elevated costs. In this context, this paper describes a strategy of optimization of the consumption. This strategy is based on a comparative study of the sinusoïdal and trapezoïdal of a permanent magnets motor conceived by a systemic approach and integrating a system of energy recuperation in order to reduce the consumption. The results gotten encourages the realization of a vehicle prototype to test the validity of the approach of conception of this power chain experimentally.

Index Terms—Electric Vehicles, Design, Control, Electromagnetic switches, Sinusoidal control, Trapezoidal control, Power chain.

1 INTRODUCTION

The electric vehicles offer the advantage of a big reduction of the atmospheric and resonant pollution. On the other hand, the production of the electric vehicles is braked again by the problem of infrastructure of refill of the batteries, their elevated cost and their weak autonomy. In this context, the study presented in this paper, treat the problem of improvement of the autonomy. Indeed, two strategies of control of the power chain (trapezoidal and sinusoïdal) are studied and compared of point of seen performances and economy of energy. The results gotten encourages the realization of a vehicle prototype to test the validity of the approach of conception of this power chain experimentally.

2 ANALYTIC DESIGN APPROACH OF POWER CHAIN

This approach is based on the calculation of dimensions of the electric motor dedicated to the traction. This approach is based on the general theorems concerning the design of an electrical device. This approach is detailed in [1], [2]. We present in this section the main design equations.

2.1 Dimensionning of the motor

The slot width of these structures is given by the following equation [1]:

$$L_{enc} = \left(\frac{D_e + D_i}{2}\right)\sin\left(\frac{1}{2}\times\left(\frac{2\times\pi}{N_d} - \alpha\times\beta\times\frac{\pi}{p}\times(1-r_{did})\right)\right) \quad (1)$$

- Souhir Tounsi, Université de sfax, Ecole Nationale d'Ingénieurs de Sfax (ENIS), Laboratoire d'Electronique et des Technologies de l'Information (LETI), BP W 3038 Sfax TUNISIE
- souhir.tounsi@isecs.rnu.tn

Where α is the report between the width of a main tooth and the width of a magnet, β is the report between a magnet and the polar step, N_d is the number of main teeth and rdid is the r_{tio} between the angular width of the inserted tooth and a main tooth. Table I illustrate the values of these coefficient:

Table 1. Values of the motor parameters

Designations	β	α	r_{did}	p	N_d
Trapezoidal configuration	1	1	0.2	4	6
Sinusoidal configuration	2/3	3/2	0.2	4	6

For the configurations with trapezoidal waveforms the height of a tooth is given by the following equation [2]:

$$H_d = \frac{3\times 2\times N_s}{2\times N_d}\times\frac{I_{dim}}{\delta}\times\frac{1}{K_f}\times\frac{1}{L_{enc}} \quad (2)$$

For the configurations with sinusoidal waveforms the height of a tooth is given by the following equation [3]:

$$H_d = \frac{3\times 2\times N_s}{2\times N_d}\times\frac{\frac{I_{dim}}{\sqrt{2}}}{\delta}\times\frac{1}{K_f}\times\frac{1}{L_{enc}} \quad (3)$$

Where K_f is the filling factor of the slots, δ is the allowable current density in the slots and I_{dim} is the current size of copper conductors. The method of calculation of the dimensionality current is retailed in [4]. The height of magnet for the two structures is given by the following relation:

$$H_a = \mu_0\times\frac{B_e}{B_r - \frac{S_a\times B_e}{S_a\times K_{fu}}}\times e \quad (4)$$

Where $K_{fu} < 1$ is the coefficient of flux losses. To avoid demagnetization of the magnets, the phase electric current

must be less than the demagnetization electric current Id [5]:

$$I_d = \left(\frac{B_r - B_c}{\mu_r} \times H_a - B_c \times K_{fu} \times e \right) \times \frac{p}{2 \times \mu_0 \times N_s} \quad (5)$$

Where B_c is the induction of demagnetization, B_r is the remanent induction of magnets and μ_0 is the permeability of air. The heights of the rotor yoke and the stator yoke are derived by applying the theorem of conservation of flux between a magnet and the rotor yoke, and between the main tooth and the stator yoke [5]:

$$H_{cr} = \frac{B_e}{B_{cr}} \times \frac{\text{Min}(S_d, S_a)}{2 \times \left(\frac{D_e - D_i}{2} \right)} \times \frac{1}{K_{fu}} \quad (6)$$

$$H_{cs} = \frac{B_e}{B_{cs}} \times \frac{\text{Min}(S_d, S_a)}{2 \times \left(\frac{D_e - D_i}{2} \right)} \quad (7)$$

Where B_{cr} and are B_{cs} respectively the induction in the rotor yoke and the stator yoke, S_d and S_a are respectively the section of a tooth and that of a magnet and K_{fu} is the flux leakage coefficient

2.2 Control parameters

The motor constant is defined by :

$$K_e = 2 \times n \times N_s \times A \times B \times B_g \quad (8)$$

For the axial flux structures A and B are given by:

$$A = \frac{D_e - D_i}{2} \quad (9)$$

$$B = \frac{D_e + D_i}{2} \quad (10)$$

Where D_e and D_i are respectively the external and the internal diameter of the axial flux motor, N_s is the number of spire per phase, n is the module number and B_g is the flux density in the air-gap. The converter's continuous voltage U_{dc} is calculated so that the vehicle can function at a maximum and stabilized speed with a weak torque undulation. The electromagnetic torque that the motor must exert at this operation point, via the mechanical power transmission system T_{Udc} (reducing + differential) is estimated by the following expression [6]:

$$T_{Udc} = \frac{P_f}{\Omega} + T_d + (T_b + T_{vb} + T_{fr}) + \frac{T_r + T_a + T_c}{r_d} \quad (11)$$

Where T_b is the rubbing torque of the motor, T_{vb} is the viscous rubbing torque of the motor, T_{fr} is the fluid rubbing torque of the motor, T_r is the torque due to the friction rolling resistance, T_a is the torque due to the aerodynamic force, T_c is the torque due to the climbing resistance, T_d is the reducer losses torque and P_f are the iron losses and Ω is the motor angular speed. At this operation point, the phase current is given by the following relation:

$$I_p = \frac{T_{Udc}}{K_e} \quad (12)$$

The only possibility making it possible to reach the current value I_p with a reduced undulation factor (10% for example) is to choose the converter's continuous voltage solution of the following equation [6]:

$$r = \frac{t_m}{t_p} = 10\% \quad (13)$$

Where t_p is the phase current maintains time at vehicle maximum speed and tm is the boarding time of the phase current from zero to I_p [6]:

$$t_m = -\frac{L}{R} \times \ln \left(1 - \frac{2 \times R \times I_p}{U_{dc} - K_e \times \Omega_{max}} \right) \quad (14)$$

Where R and L are respectively the phase resistance and inductance and Ωmax is the maximum angular velocity of the motor. The phase current maintains time at maximum speed of vehicle (corresponds to 120 electric degrees) is given by the following formula [6]:

$$t_p = \frac{1}{3} \times \frac{2 \times \pi}{p \times \Omega_{max}} \quad (15)$$

The converter's continuous voltage takes the following form:

$$U_{dc} = \frac{2 \times R \times I_p}{1 - \exp\left(-\frac{2 \times \pi \times r}{3 \times p \times \Omega_{max} \times \frac{L}{R}} \right)} + K_e \times \Omega_{max} \quad (16)$$

The converter continuous voltage increases by increasing of the vehicle speed which validates the fact of calculating its value at maximum speed. Two important factors involving the increase of the converter continuous voltage:

- The increase of the motor electric constant.
- The reduction of the undulation factor.

Consequently, a compromise between the reduction of the converter continuous voltage directly related to the space reserved for the battery and the reduction of undulation factor is to be found. The converter's continuous voltage for sinusoidal control is expressed as follow [3]:

$$U_{dc} = \frac{\pi}{2} \times \sqrt{(R \times I_p + E_{phi})^2 + (L \times p \times \Omega_{max} \times I_p)^2} \quad (17)$$

E_{phi} is the maximal value of the electromotive force to maximal speed [3]:

$$E_{phi} = \frac{2}{3} \times K_e \times \Omega_{max} \quad (18)$$

The insertion of a gear speed amplifier with rd ratio aims to enable the vehicle to reach the maximum speed of 80 km / h in our application. This ratio also helps ensure proper interpolation of reference voltages in order to have a good quality of electromagnetic torque.

$$r_d = \frac{R_r \times F_{ri}}{n_{qTA} \times V_{max} \times p \times n_{iTR}} \quad (19)$$

Where n_{iTR} is the reference voltages interpolation coefficient and V_{max} is the maximum speed of the vehicle. The leakage flux through the copper goes through about half of the copper surface, which the occurrence of the coefficient 2 in the calculation of the leakage flux reluctance in the copper. We can deduce the value of the total inductance from the following equations:

$$L = \frac{\mu_0}{2}\left(\frac{S_d}{e + H_a} + \frac{\left(\frac{D_e - D_i}{2}\right) \times H_d}{L_{enc}}\right) \times N_s^2 \quad (20)$$

Where S_d is the area of the main tooth, H_d is the height of the slot, H_a is the height of the magnet, L_{enc} is the width of the slot and e is the thickness of the air-gap The principle of the calculation of the mutual inductance is based on the supply of a coil for the calculation of the flux sensed by the adjacent coil. The flux path determines the total reluctance of the magnetic circuit modeling this mutual inductance.

$$M = \mu_0 \frac{\left(\frac{D_e - D_i}{2}\right) \times \left(\frac{D_e + D_i}{4}\right)}{4 \times (e + H_a)} N_s^2 \quad (21)$$

A_{encm} where is the average width of the slot, A_{dentm} is the average width of the main tooth, A_{dentim} is the average width of the tooth interposed, H_{cr} is the height of the rotor yoke, H_{cs} is the height of the stator yoke, μ_0 is the absolute permeability, μ_r is the relative permeability of the magnets.

2.3 Static converter

The structure of the static converter to two electro-magnet is illustrated by the following face [7]:

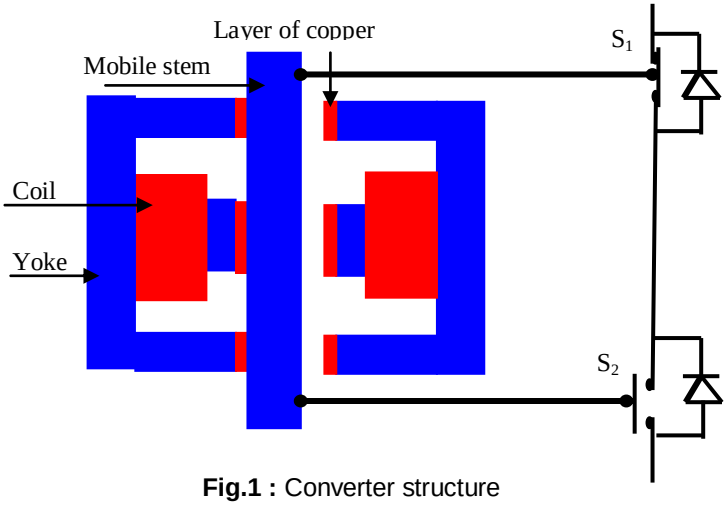

Fig.1 : Converter structure

This structure is composed of two contacts mechanical S1 and S2, one closed to rest and the other opened, to avoid the problem of short circuit. The food of the coil by a sufficient current, drag the attraction of the stem by phenomenon of induction, and thereafter the change of states of the S1 switches and S2. The dice-excitation of the coil drives to the annulment of the strength of attraction of the stem, allowing the switches to take their initial states.

3 FINITE ELEMENT VALIDATION OF THE ANALYTIC DESIGN APPROACH

3.1 Finite element model

The motor is studied on a cylindrical cut plan. The plan of cut makes itself according to the middle diameter of the motor (Fig.2), then we spreads the structure, that means the length of the cuts Lc is the perimeter of the circle according to the done cut and this next is on the middle diameter. This quantity is worth:

$$L_c = 2 \times \pi \times \left(\frac{D_e + D_i}{4}\right) \quad (22)$$

The width of a main tooth is given by the following relation:

$$L_d = A_{dentm} \times \left(\frac{D_e + D_i}{4}\right) \quad (23)$$

Where Adentm is the middle angle of opening of a main tooth. The width of a inserted tooth is given by the following relation:

$$L_d = A_{dentim} \times \left(\frac{D_e + D_i}{4}\right) \quad (24)$$

Where A_{dentim} is the middle angle of opening of a inserted tooth. The slot width is given by the following relation:

$$L_{enc} = \left(\frac{D_e + D_i}{2}\right)\sin\left(\frac{1}{2}\times\left(\frac{2\times\pi}{N_d} - \alpha\times\beta\times\frac{\pi}{p}\times\left(1 - r_{did}\right)\right)\right) \quad (25)$$

The width of a magnet is expressed by the following relation:

$$L_d = \frac{\pi}{p}\times\beta\times\left(\frac{D_e + D_i}{4}\right) \quad (26)$$

The length of the model is expressed like follows:

$$L_m = \frac{D_e - D_i}{2} \quad (27)$$

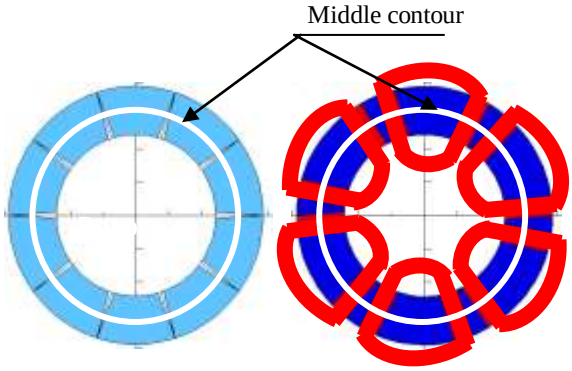

Fig.2 : Contour of the cylindrical cut

When we spreads the cylindrical cut plan, we gets the model 2 D of the motor (Figure 3).

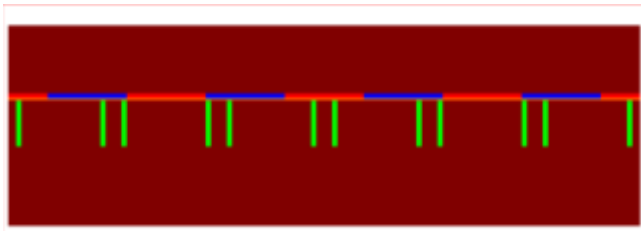

Fig.3 : 2D model of the motor

3.2 Distribution of the flux lines

The flux line at load for the trapez motor and the sinus motor are illutrated respectively by fig.4 and fig.5 [8]:

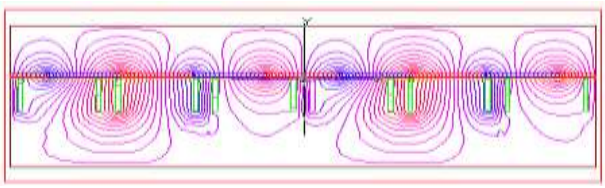

Fig.4 : Distribition of the flux line of trapeze motor

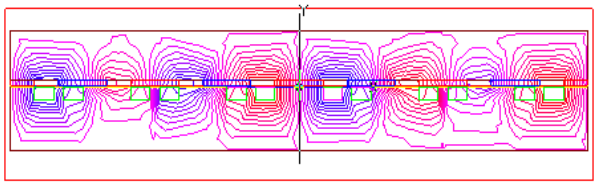

Fig.5 : Distribition of the flux line of sinus motor

The distribution of the field lines show the absence of the leakage of inter-magnets, what leads to consider that the coefficient of flux leakage is equal to 1 (Kfu=1). This property is found by optimization of the geometric parameters (e, β et α) by finite element simulations.

3.3 Simulation results

The flux at load for the motor with tarpezoïdal wave-form is illustrated by the following figure [8] :

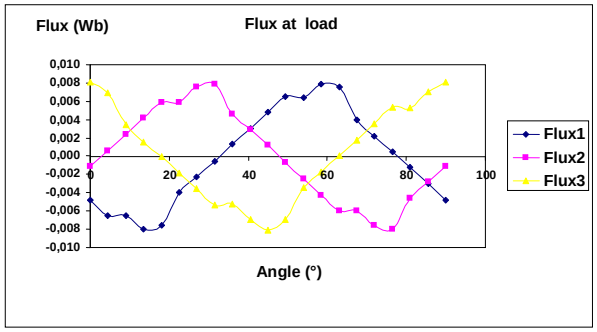

Fig.6 : Flux at load for the motor with tarpezoïdal wave-form

The flux at load for the motor with sinusoïdal wave-form is illustrated by the following figure [8] :

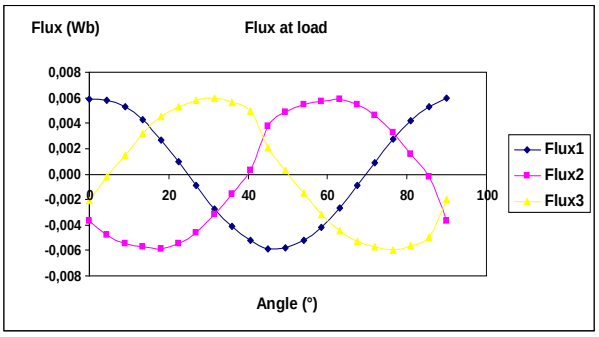

Fig.7 : Flux at load for the motor with sinusoïdal wave-form

The electromotive forces (Emf) at load for the motor with Trapezoïdal wave-form is illustrated by the following figure [8]:

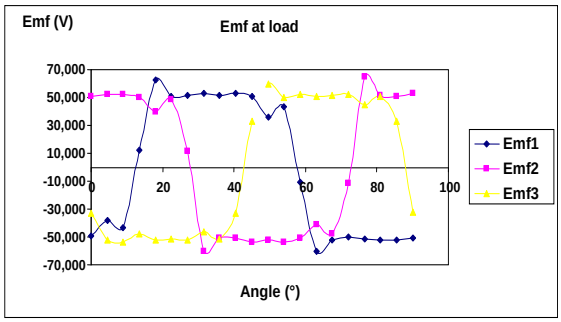

Fig.8 : Emf at load for the motor with trapezoïdal wave-form

The electromotive forces at load for the motor with sinusoïdal wave-form is illustrated by the following figure [8]:

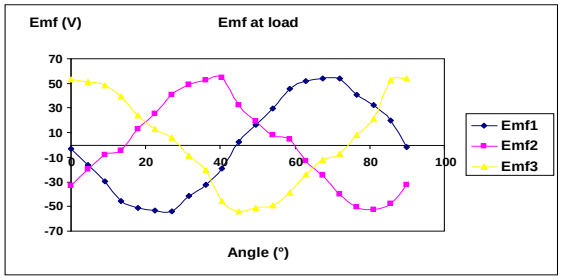

Fig.9 : Emf at load for the motor with sinusoïdal wave-form

The electromagnetic torque calculated from Emf at no load and the Emf at load for the motor with trapezoïdal wave-form is illustrated by the following figure [8] :

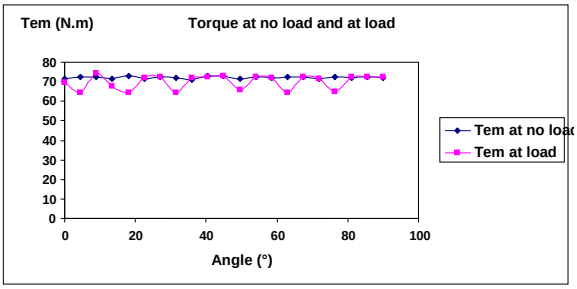

Fig.10 : Electromagnetic torque

The electromagnetic torque calculated from Emf at no load and the Emf at load for the motor with sinusoïdal wave-form is illustrated by the following figure [8]:

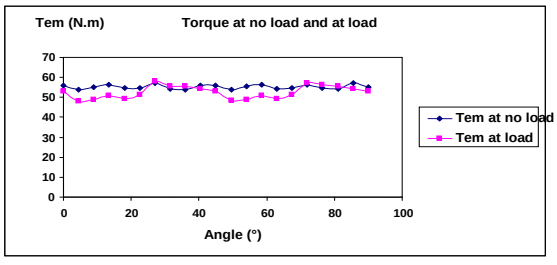

Fig.11 : Electromagnetic torque

The values of flux, Emf and torque acheive the these found by analytic calculation, what validates this design approach.

3.4 Modeling of the inductance

The inductance value is usually low for this type of machine because the flux created by the coil must cross the air-gap and the magnet thickness. In order to compute the inductance, the motor is supplied by its peak current and the magnets are replaced by air [6]. The flux lines distribution around one stator pole are illustrated by following figure:

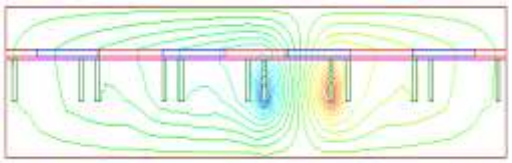

Fig. 12 . Flux lines distribution around one stator pole

The motor air-gap is relatively large producing then important flux leakages in slots. For a linear system, the inductance value of a phase constituted by two coils may be obtained from:

- The energy calculation:

$$L = \frac{2}{I^2} \times \frac{D_e - D_i}{2} \times \iint_{area} B_m \times H \times ds \qquad (28)$$

-The flux calculation :

$$L = \frac{N_s}{I} \times \frac{1}{s_{slot}} \times \frac{D_e - D_i}{2} \times \int A_s \cdot ds \qquad (29)$$

Where B_m is the flux density, H is the magnetic field, s_{slot} is the slot area and A_s is scalar potential. The finite elements analysis valid the analytic model of inductance.

4 POWER CHAIN GLOBAL MODEL

4.1 Convereter model

The converter's model rests on the comparison of the three reference voltages (trapezoidal or sinusoidal) to a triangular signal of frequency very superior to this voltages. The exits of the three comparators attack three hysteresis to reproduce the real shape of voltage delivered by the converter. The converter's model is implanted under the environment of Matlab/Simulink according to the following figure [7] :

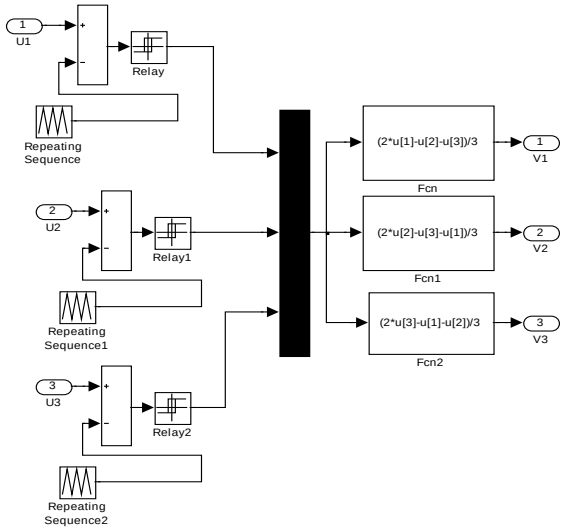

Fig.13 : Simulink model of the converter

4.1 Motor model

The phase's voltages equations of the motor with shape of waves sinusoïdals are expressed like follows:

$$u_2 = R_{t.} \times i_1 + L_t \times \frac{di_1}{dt} + \frac{K_e}{2} \times \Omega \times \cos\left(p \times \Omega \times t + \frac{\pi}{2}\right) \quad (30)$$

$$u_2 = R_{t.} \times i_2 + L_t \times \frac{di_2}{dt} + \frac{K_e}{2} \times \Omega \times \cos\left(p \times \Omega \times t - \frac{2 \times \pi}{3} + \frac{\pi}{2}\right) \quad (31)$$

$$u_3 = R_{t.} \times i_3 + L_t \times \frac{di_3}{dt} + \frac{K_e}{2} \times \Omega \times \cos\left(p \times \Omega \times t + \frac{2 \times \pi}{3} + \frac{\pi}{2}\right) \quad (32)$$

$$L_t = L - M \quad (33)$$

The electromagnetic torque is expressed by the following relation:

$$T_{em} = i_1 \times \frac{K_e}{2} \times \cos\left(p \times \Omega \times t + \frac{\pi}{2}\right) + i_2 \times \frac{K_e}{2} \times \cos\left(p \times \Omega \times t - \frac{2 \times \pi}{3} + \frac{\pi}{2}\right) + i_2 \times \frac{K_e}{2} \times \cos\left(p \times \Omega \times t + \frac{2 \times \pi}{3} + \frac{\pi}{2}\right) \quad (34)$$

The voltages and torque equations to shapes of trapezoidal waves are given in [7]. The model of the motor is implanted under the environment of Matlab/Simulink according to the following face:

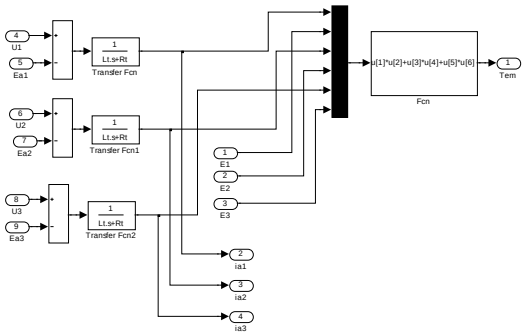

Fig.14 : Simulink model of th motor

4.2 Currents regulators

The currents regulators permit to generate the food voltage while comparing the currents with amplitude reference controled by the regulator of speed to the currents delivered by the motor. The model of the regulators of the currents implanted under the environment of Matlab/Simulink is illustrated by the following face:

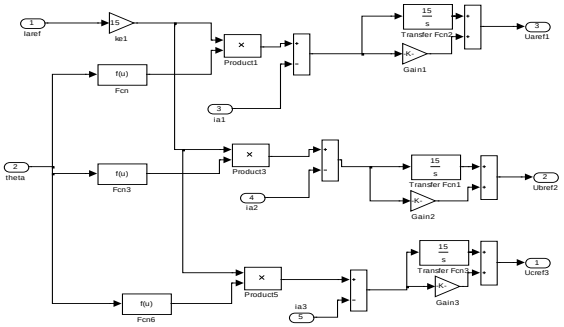

Fig.15 : Simulink model of the currents regulators

4.3 Energy recuperation system

The system of energy recuperation functions at the time of decelerations corresponding to a recoverable energy. This phase of working corresponds to a deceleration superior to a limit ψ optimized by several simulations, in order to reach a maximal recovered energy. In this phase of working, the three coils of the motor are connected to a rectifier to convert the three electromotive forces to a continuous voltage filtered by a capacity of strong value. This voltage passes by a floor of amplification (DC-DC converter of amplification report also optimized following several simulations). Finally, the amplified continuous voltage attacks the accumulator of energy until the annulment of the current (The accumulator of energy is in phase of refill: working in generating). When the current annuls itself, the coils of the motor connect to the converter (working in motor). The load volatge of the energy accumulator for a motor to sinusoïdal control is expressed by the following relation:

$$U_r = \frac{2}{3} \times K_e \times \Omega \times 3 \times \frac{\sqrt{3}}{\pi} \times \frac{1}{1-\alpha} \quad (35)$$

This quantity for the motor to trapezoidal control is expressed by the following relation:

$$U_r = \frac{2}{3} \times K_e \times \Omega \times \frac{1}{1-\alpha} \quad (36)$$

Where α is the cyclic report of the control voltage of the DC-DC elevator conveter IGBT transistor. To This phase of working, The torque on the tree motor Tm for the motor to sinusoidal control is expressed as follows:

$$T_m = -\frac{2}{3} \times K_e \times \Omega \times 3 \times \frac{\sqrt{3}}{\pi} \times \frac{1}{1-\alpha} \times \left(\frac{2}{3} \times K_e \times \Omega \times 3 \times \frac{\sqrt{3}}{\pi} \times \frac{1}{1-\alpha} - U_{batt} \right) \times \frac{1}{R_{batt}} \times \frac{1}{\Omega} \quad (37)$$

and for the motor to trapezoidal control:

$$T_m = -\frac{2}{3} \times K_e \times \Omega \times \frac{1}{1-\alpha} \times \left(\frac{2}{3} \times K_e \times \Omega \times \frac{1}{1-\alpha} - U_{batt} \right) \times \frac{1}{R_{batt}} \times \frac{1}{\Omega} \quad (38)$$

Where U_{batt} and R_{batt} are respectively the middle voltage and the resistance of the energy accumulator. Out this régime of working, the motor torque for an sinusoïdal order is:

$$T_{em} = i_1 \times \frac{K_e}{2} \times \cos\left(p \times \Omega \times t + \frac{\pi}{2} \right) + i_2 \times \frac{K_e}{2} \times \cos\left(p \times \Omega \times t - \frac{2 \times \pi}{3} + \frac{\pi}{2} \right) + i_2 \times \frac{K_e}{2} \times \cos\left(p \times \Omega \times t + \frac{2 \times \pi}{3} + \frac{\pi}{2} \right) \quad (39)$$

For the trapezoidal order, this torque is given in [9].

4.4 Global model with energy recuperation system

The coupling of the different models of the electric vehicle power chain leads to the global model implanted under the environment of Matlab/Simulink (7.1 vesion) according to the Figure 16:

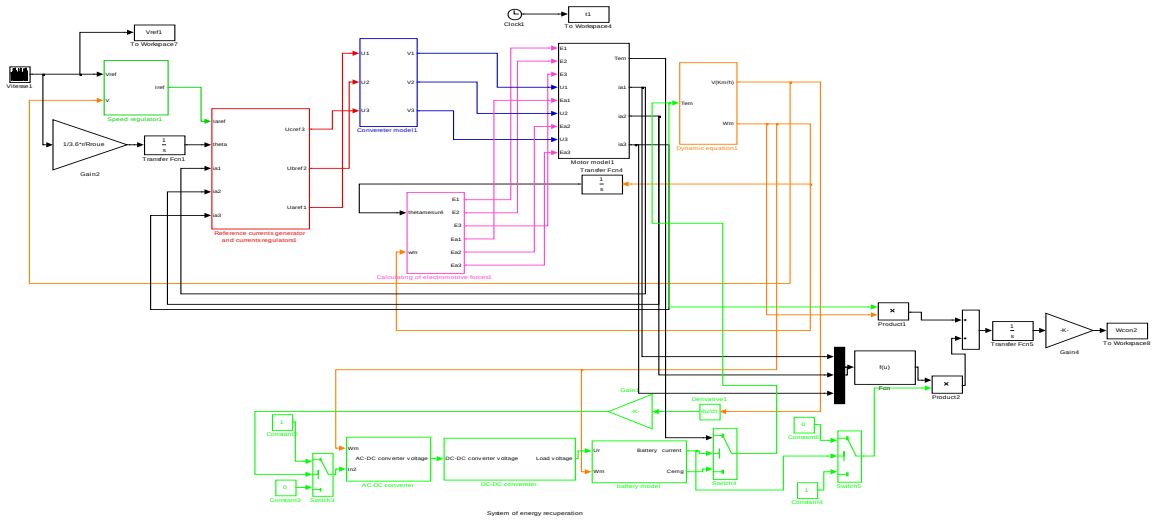

Fig.16 : Global model with energy recuperation system

5 SIMULATIONS RESULTS

The response of speed to the speed of reference in the two cases is illustrated by the following face:

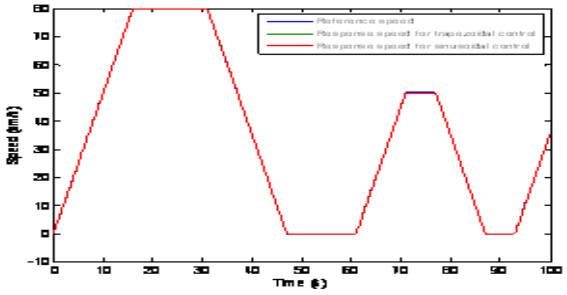

Fig.17 : Speed responses

This face shows the good dynamic characteristic and valid thereafter the approach of design of the two power chains. The current of phase in the two case is illustrated by the face following:

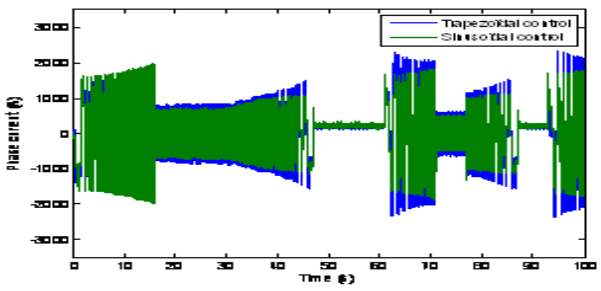

Fig.18 : Phase current

This face shows that the currents are comparable, what proves the setting in equivalence of the two structures of power chains. This face also shows that the current of starting is weak for the two structures what shows the performance of the two chosen control techniques. The following face illustrates the evolutions of the currents of phase for the two chains of powers :

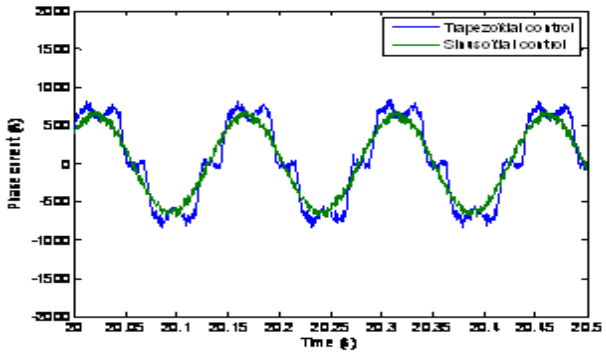

Fig.19 : Wave-form of the phase current

For the trapeze control, the pace of the current is very close to a trapezoidal shape. For the sinus control, the pace of the current is close to a sinusoïdal shape. This shows the performance of the two techniques of control chosen. The following face illustrates the responses of speed to a normalized browses in the two cases of configuration.

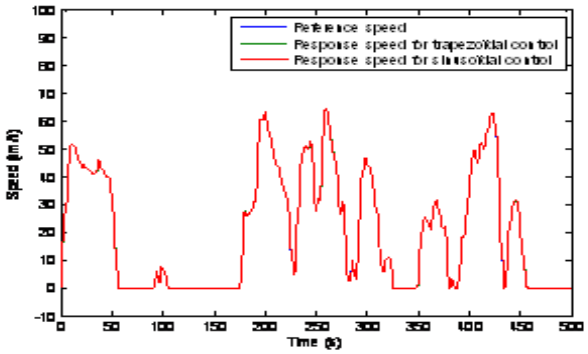

Fig.20 : Responses speed

This face also shows the performance of the two techniques of control chosen. The evolutions of the energy consumed in the two cases are illustrated by the following face:

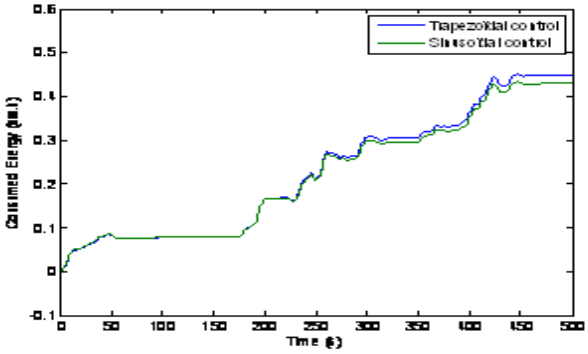

Fig.21 : Consumed energy

This face shows that the energies consumed in the two cases are comparable. The following face illustrates the evolutions of the energies recovered in the two cases of configuration:

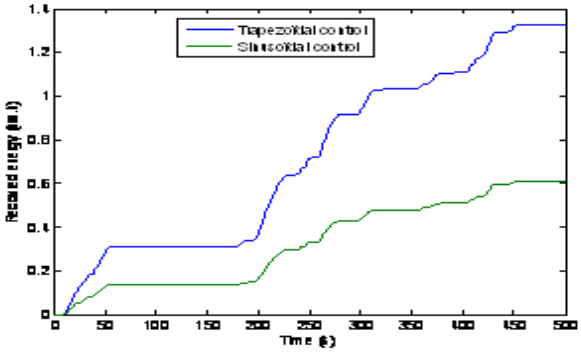

Fig.22 : Recovred energy

This face shows that the energy recovered in the case sinus is distinctly weaker than the one in The case trapeze. This energy is of values respective Ws=0.3276 kw.h and Wt=0.7151 kw.h.

6 Conclusion

In this paper, we present a comparative study between a power chain to trapezoidal control and another to sinusoïdalontrol. The design approach of the two chains of power is presented briefly. A validation study the design approach the finite element method is also presented. The study of the two power chains performances, following a modelling under the environment of Mtalab/Simulink, watch that these two chain power is comparable and presents an attractive solution for the problem of motorization of the electric vehicles.

Reference

[1] R. NEJI, S. TOUNSI et F. SELLAMI: “Contribution to the definition of a permanent magnet motor with reduced production cost for the electrical vehicle propulsion”, European Transactions on Electrical Power (ETEP), 2006, 16: pp. 437-460.

[2] S. TOUNSI, R. NEJI et F. SELLAMI: “Conception d’un actionneur à aimants permanents pour véhicules électriques” Revue Internationale de Génie Electrique (RIGE), Volume 9 – n° 6/2006, pp. 693-718.

[3] R. NEJI, S. TOUNSI, F. SELLAMI: “Optimization and Design for a Radial Flux Permanent Magnet Motor for Electric Vehicle”, Journal of Electrical Systems, Volume 1, isuue 4 (2005), pp. 47-68.

[4] S. TOUNSI, R. NEJI, and F. SELLAMI: “Design Methodology of Permanent Magnet Motors Improving Performances of Electric Vehicles”, International Journal of Modelling and Simulation (IJMS), Volume 29, N° 1, 2009.

[5] S. Tounsi, R. Neji et F. Sellami: “Design of a radial flux permanent magnet motor for electric vehicle”,

10th European Conference on Power lectronics and Applications (EPE 2003), 2-4 September, Toulouse, France.

[6] S. TOUNSI et R. NEJI: “Design of an Axial Flux Brushless DC Motor with Concentrated Winding for Electric Vehicles”, Journal of Electrical Engineering (JEE), Volume 10, 2010 - Edition: 2, pp. 134-146.

[7] M. HADJ KACEM, S. TOUNSI and Rafik NEJI: “Systemic Design and control of Electric Vehicles Power Chain”, **IJSTR journal November 2012 edition.**

[8] N. Mellouli, S. Tounsi et R. Neji: “Modelling by the finite elements method of a coiled rotor synchronous motor equivalent to a permanent magnets axial flux motor”, 1nd International Conference on Electrical Systems Design & Technologies (ICEEDT’07), 4-6 Novembre 2007, Hammamet, TUNISIA.

[9] S. TOUNSI « Control of the Electric Vehicles Power Chain with Electromagnetic Switches Reducing the Energy Consumption», Journal of Electromagnetic Analysis and Applications, Volume 3 N° 12, December 2011.